

Synthesis and Reactions of *fac*-[Re(dmbpy)(CO)₃X] (dmbpy = 4,4'-Dimethyl-2,2'-bipyridine; X = COOH, CHO) and Their Derivatives

Dorothy H. Gibson,* Xiaolong Yin, Haiyang He, and Mark S. Mashuta

Department of Chemistry, University of Louisville, Louisville, Kentucky 40292

Received August 19, 2002

Reactions of *fac*-[Re(dmbpy)(CO)₃COOH] (**1**) alone or together with *fac*-[Re(dmbpy)(CO)₃CHO] (**4**) or other compounds which could be generated in photocatalytic reductions of CO₂ from *fac*-[Re(dmbpy)(CO)₃Cl] have been studied to establish possible routes to CO and formate. The results suggest that the reactions of **1** are governed by complex equilibria involving its ionization to Re(dmbpy)(CO)₄⁺ and OH⁻ or proton transfer to highly basic species. Parallel reaction paths, emanating from Re(dmbpy)(CO)₄⁺, are suggested to account for the formation of CO and formate in the catalytic reactions and support the proposal that **4** is a likely catalytic intermediate in addition to **1**. New compounds have been isolated or prepared in order to support proposals about reaction pathways: {*fac*-[Re(dmbpy)(CO)₃]₂-(OCO₂)} (**5**), *fac*-[Re(dmbpy)(CO)₃OH]·2.5H₂O (**8a**), {*fac, fac*-[Re(dmbpy)(CO)₃]₂(H)}[OTf] (**11**), *fac, fac*-[Re(dmbpy)(CO)₃CO₂Re(bpy)(CO)₃] (**13**), *fac*-[Re(bpy)(CO)₃OH] (**17**) and {*fac, fac, fac*-[Re(dmbpy)(CO)₃]₃(OCO₂)}[ReO₄] (**18**). Compounds **8a** and **18** have been characterized by X-ray crystallography.

Introduction

Rhenium complexes with polypyridine ligands are of interest because of the role of these compounds in photo- and electrocatalytic reductions of CO₂.¹ Photocatalytic reductions of CO₂ using *fac*-[Re(N–N)(CO)₃Cl] (N–N = bidentate bipyridine ligand) yield CO and formate. Metalcarboxylic acids (M–COOH) have been proposed as intermediates in the production of CO, but the origin of formate has remained obscure. We have reported the synthesis and preliminary results on reactions of *fac*-[Re(dmbpy)(CO)₃COOH] (**1**; dmbpy = 4,4'-dimethyl-2,2'-bipyridine)² which indicated that it is not a likely source of formate in the catalytic reactions, although it could certainly be the source of CO. In the absence of CO₂, the major reaction product from the acid in either DMF-*d*₇ or DMSO-*d*₆ was the bridged compound *fac, fac*-[Re(dmbpy)(CO)₃CO₂Re(dmbpy)(CO)₃] (**2**); in the presence of CO₂, the major product was the bicarbonato complex *fac*-[Re(dmbpy)(CO)₃OCO₂H] (**3**). More recently, we have reported the synthesis and some reactions of the related formyl complex *fac*-[Re(dmbpy)(CO)₃CHO] (**4**)

and provided results which argue for its intermediacy in the catalytic reactions as a viable source of the observed formate product.³ Since product mixtures in the catalytic reactions could include **1** and **4**, a fuller study of their interactions with one another as well as the reactions of **1** with compounds that could be derived from it under the catalytic conditions was warranted. A complete list of compounds required in this study is shown in Chart 1.

Results and Discussion

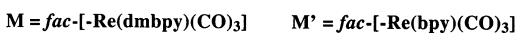
In previous work we noted the lability of **1** in solution at room temperature in either DMSO-*d*₆ or DMF-*d*₇.² In preparative reactions, samples of the acid allowed to stand for a short time, followed by solvent removal (DMF) under vacuum or longer standing (DMSO, 2 h) followed by purging with N₂, afforded the CO₂-bridged compound **2** as the major reaction product in 63–73% yields. Other products, in small amounts, were also evident; a 10% yield of the bicarbonato complex **3** was reported previously from reactions in DMSO-*d*₆. In addition, a small amount of an insoluble compound was formed in that reaction, which was not characterized. The progress of reactions in both solvents was followed over time by ¹H NMR spectroscopy. Rapid transformation of **1** took place in DMF-*d*₇ to give a reaction intermediate that closely resembled **2** except for the broadening of two resonances as reported earlier; after prolonged standing, the major product was **2**. Reactions of **1** in DMSO-*d*₆ were slower but also generated an intermediate species with spectral properties closely resembling those of **2**; over time, these reactions generated the same products together with a small amount

(1) (a) Hawecker, J.; Lehn, J. M.; Ziessel, R. *J. Chem. Soc., Chem. Commun.* **1983**, 536. (b) Sullivan, B. P.; Bolinger, C. M.; Conrad, D.; Vining, T. J.; Meyer, T. J. *J. Chem. Soc., Chem. Commun.* **1985**, 1414. (c) Sullivan, B. P.; Conrad, D.; Meyer, T. J. *Inorg. Chem.* **1985**, *24*, 3640. (d) Hawecker, J.; Lehn, J.-M.; Ziessel, R. *Helv. Chim. Acta* **1986**, *69*, 1990. (e) Ziessel, R. In *Catalysis by Metal Complexes: Photosensitization and Photocatalysis Using Inorganic and Organometallic Compounds*; Kalyanasundaram, K., Grätzel, M., Eds.; Kluwer Academic: Dordrecht, The Netherlands, 1993; p 217. (f) Christensen, P.; Hamnett, A.; Mui, A. V. G.; Timney, J. A. *J. Chem. Soc., Dalton Trans.* **1992**, 1455. (g) Stor, G. J.; Hartl, F.; van Outersterp, J. W. M.; Stufkens, D. J. *Organometallics* **1995**, *14*, 115. (h) Johnson, F. P. A.; George, M. W.; Hartl, F.; Turner, J. J. *Organometallics* **1996**, *15*, 3374. (i) Klein, A.; Vogler, C.; Kaim, W. *Organometallics* **1996**, *15*, 236. (j) Scheiring, T.; Klein, A.; Kaim, W. *J. Chem. Soc., Perkin Trans. 2* **1997**, 2569.

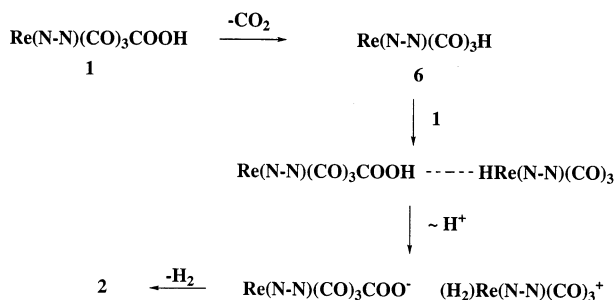
(2) (a) Gibson, D. H.; Yin, X. *J. Am. Chem. Soc.* **1998**, *120*, 11200. (b) Gibson, D. H.; Yin, X. *J. Chem. Soc., Chem. Commun.* **1999**, 1411.

(3) Gibson, D. H.; He, H. *J. Chem. Soc., Chem. Commun.* **2001**, 2082.

Chart 1. Compound Formulas



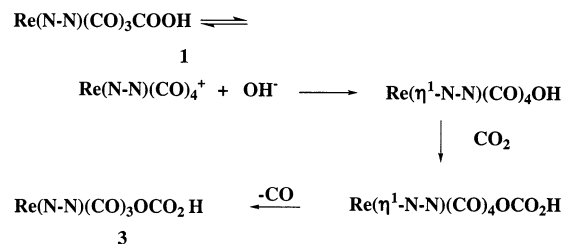
compound number	compound type	X
1	M-X	-COOH
2	M-X-M	-CO ₂ -
3	M-X	-OCO ₂ H
4	M-X	-CHO
5	M-X-M	-OCO ₂ -
6	M-X	-H
7	M-X	-OCHO
8a	M-X·2.5 H ₂ O	-OH
8b	M-X·H ₂ O	-OH
9a	M-X ⁺ , OTf ⁻	-CO
9b	M-X ⁺ , BF ₄ ⁻	-CO
10	MX	-M
11	MX ⁺ , OTf ⁻	-HM
12	M'-X	-H
13	M-X-M'	-CO ₂ -
14	M'-X	-OCHO
15	M-X	-OTf
16	M'-X	-OTf
17	M'-X	-OH
18	M ₃ X ⁺ , ReO ₄ ⁻	-OC(O-)O-

Scheme 1^a

^a N-N = 4,4'-dimethyl-2,2'-bipyridine.

of an insoluble compound which has now been identified as the carbonato-bridged compound *fac, fac*-{[Re(dmbpy)(CO)₃]₂OCO₂} (**5**) (vide infra). The reactions conducted in DMF-*d*₇ did not provide this product.

In trying to establish how the conversions of **1** to **2** took place, we conducted experiments previously with equimolar quantities of acid **2** and the related hydride *fac*-[Re(dmbpy)(CO)₃H] (**6**) in both solvents.^{2a} In both cases, an intermediate species closely resembling the one generated from **1** alone was generated in these solutions after a few minutes. These reactions eventually afforded **2**, small amounts of bicarbonato complex **3**, and a small amount of formate complex (**7**) in the DMF reaction. On the basis of these results, we proposed that the main pathway for conversion of the acid to **2** involved the sequence shown in Scheme 1; the presence of both **3** and **7** in the reaction mixture seemed to support this pathway (both require loss of CO₂ from **1**). In our recent experiments, we have attempted to standardize conditions in order to probe, in greater

Scheme 2^a

^a N-N = 4,4'-dimethyl-2,2'-bipyridine.

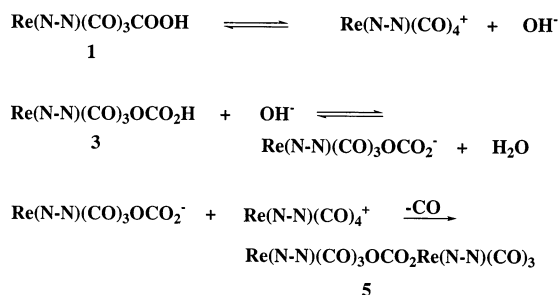
detail, the reactions of **1** alone and those involving the acid together with **6** and with other species which might be present in DMF under catalytic conditions.

(a) Reactions of **1** and **2** with CO₂ in DMSO-*d*₆.

In previous work we noted that, after purging solutions of the acid (**1**) in DMSO-*d*₆ with CO₂ and allowing the sample to stand for several hours, bicarbonato compound **3** was obtained in high yield.^{2b} The progress of the experiment was not followed over time. It was also observed previously that purging a solution of the CO₂-bridged compound **2** with CO₂ and allowing the solution to stand for about 10 min afforded approximately equal amounts of the bicarbonato compound and the acid. We rationalized these products as resulting from hydrolysis of **2** followed by CO₂ insertion into *fac*-[Re(dmbpy)(CO)₃OH]·H₂O (**8b**); the latter reaction had been shown to occur quickly.^{2b} Recently, however, we have compared the rates of reactions of acid **1** and the CO₂-bridged compound **2** with CO₂ under comparable conditions and followed the progress of the reactions over time by ¹H NMR. After only 10 min, the sample from the acid consisted of 42% bicarbonato compound **3** and 58% unreacted acid. In contrast, the sample from the CO₂-bridged compound showed 21% **3**, 15% **1**, and 64% unreacted **2**. After reaction times of 20 min, the sample prepared from the acid consisted of 70% **3** and 30% unreacted **1**, while the sample from the CO₂-bridged compound consisted of 38% **3**, 11% **1**, and 51% unreacted **2**. These results clearly indicated to us that a pathway exists for conversion of the acid to **3** that does not involve prior conversion of **1** to **2**. A possible explanation for this behavior is that the acid establishes equilibrium with a hydroxo complex that is rapidly converted to **3** upon exposure to CO₂, as illustrated in Scheme 2 and discussed below.

In the initial study of the reactions of **1** in DMSO-*d*₆, we obtained small amounts of an insoluble compound which has now been identified as the carbonato-bridged compound **5** (see below for the characterization of **5**); this product was not obtained in the DMF reactions involving **1** alone, but small amounts of bicarbonate **3** were found in those reactions. We determined that **5** can be formed by mixing equimolar quantities of **3** and [Re(dmbpy)(CO)₄][OTf] (**9a**)⁴ in DMF-*d*₇ followed by aqueous KOH; compound **5** appeared after 30 min and became the main product. Clearly, the formation of **5** required **3**, OH⁻, and Re(dmbpy)(CO)₄⁺. As shown in Scheme 3, dissociation of **1** could provide the necessary ions; with the additional presence of **3**, **5** could be formed. The fact that **5** was formed from **1** only in DMSO solutions may be due to differences in solubility;

(4) Shaver, R. J.; Rillema, D. P. *Inorg. Chem.* **1992**, *31*, 4101.

Scheme 3^a

^a N-N = 4,4'-dimethyl-2,2'-bipyridine.

it is sparingly soluble in DMF but nearly insoluble in DMSO. In this solvent, the equilibrium involving the acid and its two ions (shown in Scheme 3) would shift to the right as **5** begins to precipitate, thus providing a means to increase the amount of **5**. As expected, mixing equimolar quantities of **1** and **3** in DMSO led to a preparative route to **5** (see below).

(b) Reactions of 1 and 4 in DMF-*d*₇ without Other Complexes. All transformations of acid **1** described in this section, and in section c below, were done in the same way to allow comparisons: samples were prepared in a glovebox, under dry N₂, in DMF-*d*₇ (together with ferrocene as an internal standard) which had been degassed by pumping under vacuum. In a small-scale reaction with **1**, examination of the ¹H NMR spectrum of a sample produced from **1** showed that the intermediate species had formed, but broadened peaks for **1** could still be seen in ¹H NMR spectra. After 2 h, the intermediate persisted and all traces of **1** were gone. The reaction was quenched by pouring the NMR sample into a flask filled with dry N₂ and then reanalyzed by ¹H NMR. The reaction mixture consisted of 68% **2**, 10% **3**, 3% of fac,fac-[Re(dmbpy)(CO)₃]₂ (**10**),⁵ and 3% free dmbpy; there was no evidence for the carbonato-bridged complex **5**. Several reactions of **1** were done in the same way, and the results were reproduced.

A larger scale reaction of **1** in degassed DMF-*d*₇ was done so that we could probe for H₂ and CO. The reaction mixture was allowed to stand for 19 h, and then headspace analysis of the gases was done by gas chromatography: no H₂ could be detected, and less than 1 molar equiv of CO was detected. ¹H NMR analysis of the solution showed 75% **2**, 14% **5**, and much smaller amounts of several other products.

In a small-scale experiment with formyl complex **4** in degassed DMF-*d*₇, we found that **4** is relatively robust in solution in comparison with **1**. After 1 h, 95% of the formyl complex remained unchanged. After 3 h, 83% of the formyl complex remained unreacted; small amounts of **1**, **2**, hydride **6**, and formate **7** were present in the mixture.

(c) Reactions of 1 in DMF-*d*₇ with Other Compounds. Since some variation in product mixtures has been observed when different reaction conditions were used, we adopted a standardized procedure for all of the experiments in DMF-*d*₇. In each of the experiments described below, the samples (typically containing about 4 mg of **1** together with equimolar amounts of the second compound) were prepared in a glovebox under N₂ and

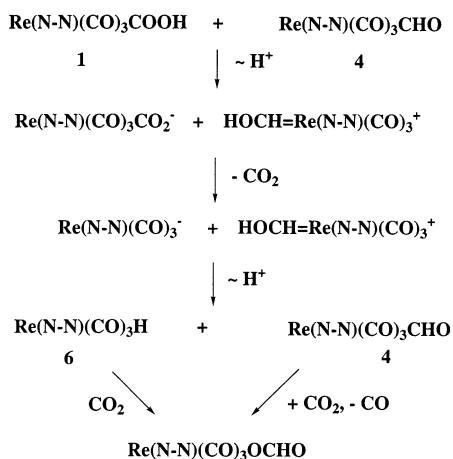
in degassed DMF-*d*₇, as were the reactions in part b above. In each case, a reaction intermediate appeared which had ¹H NMR spectral properties that were closely similar to those of the intermediate generated in reactions of **1** alone. After this intermediate appeared, and the peaks for starting materials had disappeared, reactions were quenched with N₂ as described above for the reactions of the acid alone. This group of reactions required 40 min to 3 h for completion.

Previously, we described a low-temperature reaction of **1** with an equimolar quantity of the hydroxo complex fac-[Re(dmbpy)(CO)₃OH]·H₂O (**8b**) (the orange form of the compound;^{2a} the yellow form, **8a**, is discussed below) in CH₂Cl₂ which afforded a good synthetic route to the CO₂-bridged compound **2** (90% yield).^{2a} We have now examined the reactions of the hydroxo complex **8b** with **1** in DMF-*d*₇ for comparison with other reactions involving **1** because of the possible intermediacy of hydroxo complexes in the catalytic reactions (see Scheme 2). Reaction of equimolar quantities of **1** and **8b** occurred quickly at room temperature in DMF-*d*₇. A ¹H NMR pattern that was closely similar to that observed for the reaction intermediate generated from **1** alone appeared in this reaction mixture as the main component together with a small amount of carbonato-bridged compound **5**. After 40 min and quenching with N₂, the ¹H NMR spectrum showed a product mixture consisting of the following compounds: 58% **2**, 14% of carbonato-bridged compound **5**, 10% dimer **10**, 9% of **3**, and 5% dmbpy. The significant amount of carbonato-bridged compound **5** in this reaction mixture was not initially understood. It occurred to us, on the basis of the observations of Bergman et al.⁶ about the nucleophilicity of some other hydroxo complexes toward carbonyl compounds, that **5** might be formed as a secondary product from the reaction of **2** with **8b**; however, an attempted reaction between these two compounds failed to produce **5**. Additionally, we have tried other possible routes to **5** in DMF-*d*₇ from species which could be present in the reaction mixture involving **1** and **8b**: attempted reactions of bicarbonato compound **3** and [Re(dmbpy)(CO)₄]-[OTf] (**9a**; **9b** if the anion is BF₄⁻) or between hydride **6** and **3** also failed. However, when equimolar quantities of **3**, cation **9a**, and KOH were mixed in DMF-*d*₇, compound **5** was formed within 30 min. The formation of **3** in the reaction involving **1** and **8b** can be rationalized as the result of CO₂ insertion into **8b**; partial decarboxylation of the acid to hydride **6** is the likely source of CO₂. The further conversion of **3** to **5** requires products from the ionization of **1** (Re(dmbpy)(CO)₄⁺ and OH⁻) in addition, and metalloacids are known to establish equilibrium with the ions in polar solvents.⁷ Reaction of **3** and **1** in DMSO gave **5** (65% yield, see Experimental Section). In view of these results and the results of the reactions of **1** and **2** with CO₂ in DMSO, we suggest that **2** is formed in the DMF reactions primarily by direct reaction of **1** with **8b** (or the η¹ complex indicated in Scheme 2). The remainder could be formed by reaction of **1** with **6** (see discussion below). Both dimer **10** and dmbpy are degradation products of **8b**. No bicarbonato product was reported in the photo-

(6) See: Fulton, J. R.; Holland, A. W.; Fox, D. J.; Bergman, R. G. *Acc. Chem. Res.* **2002**, *35*, 44 and references therein.

(7) Bennett, M. A. *J. Mol. Catal.* **1987**, *41*, 1.

(5) Identified by comparison with an authentic sample; see ref 1b.

Scheme 4^a

^a N-N = 4,4'-dimethyl-2,2'-bipyridine.

catalytic reactions,^{1e} although it is possible that small amounts of this product were formed and not detected.

Earlier, we reported that the reaction of **1** with the formyl complex **4** afforded the same type of intermediate product that is generated from **1** alone.³ However, the further development of this product mixture was not explored at that time. We have repeated this reaction, under the standardized conditions described above, and followed its progress with ¹H NMR spectroscopy to conclusion. Although approximately equimolar quantities of the two compounds were used, all resonances for the formyl complex had disappeared by the time the first spectrum was recorded (10 min); lower intensity resonances at the positions characteristic of acid **1** were all broadened, and resonances for the intermediate species were present as well. After 100 min, the reaction was quenched and ¹H NMR analysis performed. At this time the composition (mol %) of the mixture was as follows: 29% CO₂-bridged compound **2**, 22% formate **7**, 30% hydride **6**, 11% *fac, fac*-[Re(dmbpy)(CO)₃]₂H⁺ (cation from **11**, identified by comparison of the ¹H NMR spectrum with that of compound **11** generated from the reaction of **6** with **9a**; see Experimental Section), 5% free dmbpy, and about 1% of the rhenium dimer **10**. We suggest that the major pathways operating in the reaction of **1** with **4** are those shown in Scheme 4. Hydride **6** is known⁸ to react with CO₂ to produce formate **7**; also, we showed previously³ that **4** will transfer hydride to CO₂ rapidly and yield **7** after loss of CO. Reactions of protonic acids with formyl complexes are known to yield hydroxymethylidene cations.⁹ Also, many metalcarboxylate anions will readily decarboxylate¹⁰ to the metallo anion. Deprotonation of a hydroxymethylidene cation by strong base is also preceded.⁹ We have also shown, from a larger-scale reaction (see Experimental Section), that the reaction of **1** with **4** yields a small amount of H₂, suggesting that there is a competing reaction involving direct hydride transfer from **4** to **1** that is also responsible for some of **2**. Additional **2** may be formed from reaction of the

metalcarboxylate anion (Scheme 4) with Re(dmbpy)-(CO)₄⁺ produced by ionization of **1**; in that case, the hydroxymethylidene cation could give up a proton to OH⁻. A larger scale reaction of **1** with **4** was conducted in degassed DMF-*d*₇ in order to probe for H₂, but only a very small amount of the gas could be detected.

Reaction of equimolar quantities of **1** and hydride **6** was conducted in the same way. After 3 h, the acid was consumed and the intermediate was fully formed. After quenching, the product mixture consisted of the following compounds: CO₂-bridged compound **2** (18%), formate **7** (19%), hydride **6** (46%), 9% *fac, fac*-[Re(dmbpy)-(CO)₃]₂H⁺ (cation from **11**), free dmbpy (4%), and a trace of dimer **10**. These results were reproduced in a second experiment conducted in the same way. Since much hydride **6** remained in the final product mixture described above, we began to question whether any of **2** was actually formed by the direct reaction between **1** and **6** as suggested in Scheme 1. To answer this question, and because our method for H₂ detection was not highly sensitive, we conducted a reaction between **1** and *fac*-[Re(bpy)(CO)₃H] (**12**)⁸ in DMF-*d*₇ in the same way as the reaction between **1** and **6**. After quenching, the new product mixture consisted of *fac*-[Re(dmbpy)-(CO)₃CO₂Re(bpy)(CO)₃] (**13**; 24%, identified by comparison with an authentic sample, see below), hydride **6** (17%), formate **7** (8%), hydride **12** (17%), *fac*-[Re(bpy)-(CO)₃OCHO]⁸ (**14**, 9%), **2** (5%), and smaller amounts of several other compounds. The fact that the mixed CO₂-bridged compound **13** was the major product of the reaction certainly shows that there is direct reaction between acid and hydride. The presence of hydride **6** and formate **7**, in addition to **14**, provides further support that decarboxylation of **1** does occur. The suggested paths leading to the major products in the reaction are shown in Scheme 5. Hydridic hydrides, such as **6** (and **12**), are known to react with weakly acidic hydroxylic species, yielding dihydrogen complexes.¹¹ Also, cationic dihydrogen complexes, such as the intermediate shown, are known to be proton sources.¹²

The failure to detect any H₂ from reactions of **1** alone combined with the observation that **1** reacts slowly with **6** as compared to its reaction with **8b** suggests that the pathway shown in Scheme 1 is probably not the major path leading to **2** in reactions of **1** alone. The major path leading to **2** more likely involves the reaction of **1** with a hydroxo intermediate (**8b** or the η¹ species shown in Scheme 2). However, the experiment between **1** and hydride **12** suggests that some **2** could be formed according to Scheme 1.

(11) See, for example: Lee, J. C., Jr.; Peris, E.; Rheingold, A. L.; Crabtree, R. H. *J. Am. Chem. Soc.* **1994**, *116*, 11014. Yao, W.; Crabtree, R. H. *Inorg. Chem.* **1996**, *35*, 3007. Lough, A. J.; Park, S.; Ramachandran, R.; Morris, R. H. *J. Am. Chem. Soc.* **1994**, *116*, 8356. Park, S.; Lough, A. J.; Morris, R. H. *Inorg. Chem.* **1996**, *35*, 3001. Shubina, E. S.; Belkova, N. V.; Krylov, A. N.; Vorontsov, E. V.; Epstein, L. M.; Gusev, D. G.; Niedermann, M.; Berke, H. *J. Am. Chem. Soc.* **1996**, *118*, 1105. Ayllón, J. A.; Gervaux, C.; Sabo-Etienne, S.; Chaudret, B. *Organometallics* **1997**, *16*, 2000. Belkova, N. V.; Shubina, E. S.; Ionidis, A. V.; Epstein, L. M.; Jacobsen, H.; Messmer, A.; Berke, H. *Inorg. Chem.* **1997**, *36*, 1522. Shubina, E. S.; Belkova, N. V.; Bakhmutova, E. V.; Vorontsov, E. V.; Bakhmutov, V. I.; Ionidis, A. V.; Bianchini, C.; Marvelli, L.; Peruzzini, M.; Epstein, L. *Inorg. Chim. Acta* **1998**, *280*, 302.

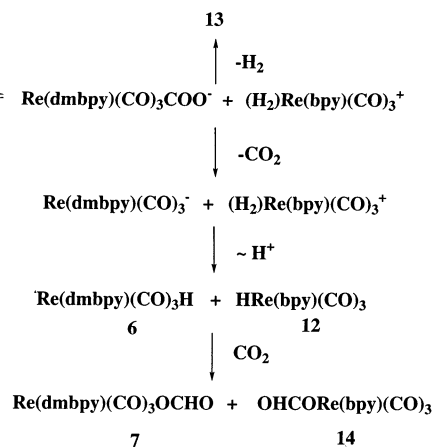
(12) (a) Kristjándóttir, S. S.; Norton, J. R. In *Transition Metal Hydrides*; Dedieu, A., Ed.; Wiley-Interscience: New York, 1992; Chapter 9. (b) Heinekey, D. M.; Oldham, W. J., Jr. *Chem. Rev.* **1993**, *93*, 913.

(8) Sullivan, B. P.; Meyer, T. J. *Organometallics* **1986**, *5*, 1500.

(9) (a) Gladysz, J. A. *Adv. Organomet. Chem.* **1982**, *20*, 1. (b) Gibson, D. H.; Mandal, S. K.; Owens, K.; Richardson, J. F. *Organometallics* **1990**, *9*, 1936.

(10) See: Gibson, D. H. *Chem. Rev.* **1996**, *96*, 2063 and references therein.

Scheme 5



(d) Other Reactions. In studying the characteristics of formyl complex **4**, one of the reactions explored was an oxidation. A sample of **4** was added to benzene, and the mixture was bubbled with O₂ and then stirred overnight. During this time, a yellow precipitate formed which was collected; the product was characterized by elemental analysis, IR and ¹H NMR spectroscopy, and X-ray crystallography. It is a trinuclear compound with a fully bridged carbonato ligand: fac, fac, fac-{[Re(dmbpy)(CO)₃](OCO₂)}₃[ReO₄] (**18**). Surprisingly, the compound was formed in 36% yield by the oxidation of **4**; we have not yet determined how **4** is converted to **18**. Compound **18** can also be synthesized from **5** (see below).

(e) Synthesis and Characterization of New Compounds. Compound **5** can be synthesized on a preparative scale by the reaction of **1** and **3** in DMSO. Compound **5** precipitated from the reaction mixture over 3.5 h and was obtained in 65% yield after washing with ether and hexane and then drying under vacuum. It was characterized by elemental analysis and by IR and ¹H NMR data. Compound **5** is not sufficiently soluble in either DMSO or DMF to obtain ¹³C NMR data. However, its structure can be inferred from its conversion to **18**. Reaction of **5** with fac-[Re(dmbpy)(CO)₃OTf] (**15**)⁴ followed by anion exchange of triflate for perrhenate afforded **18** in high yield; **18** has been structurally characterized (see below).

In earlier work,^{2a} we reported the synthesis of the orange compound fac-[Re(dmbpy)(CO)₃OH]·H₂O (**8b**). At that time, we also reported that this product was obtained after drying the initial reaction product (yellow, **8a**) under vacuum. Elemental analysis of **8a** indicated that 2.5 water molecules were associated with the compound; the spectral properties of the compound were closely similar to those of **8b**. We have now obtained structural data on **8a**, which helps to characterize both forms. The ORTEP diagram for **8a** is shown in Figure 1; crystallographic data are summarized in Table 1. Selected bond distances and bond angles are shown in Table 2. Compound **8a** exhibits distorted-octahedral geometry at the rhenium center. The Re–O bond length is 2.132(3) Å. The oxygen of the hydroxy group is bonded to two water molecules through intermolecular hydrogen bonding, with an O(1)–H(21a) separation of 1.92(6) Å and an O(1)–H(21a)–O(21) bond angle of 163.9(15)°, and with an O(1)–H(20b) separation of 1.78(6) Å and an O(1)–H(20b)–O(20) bond

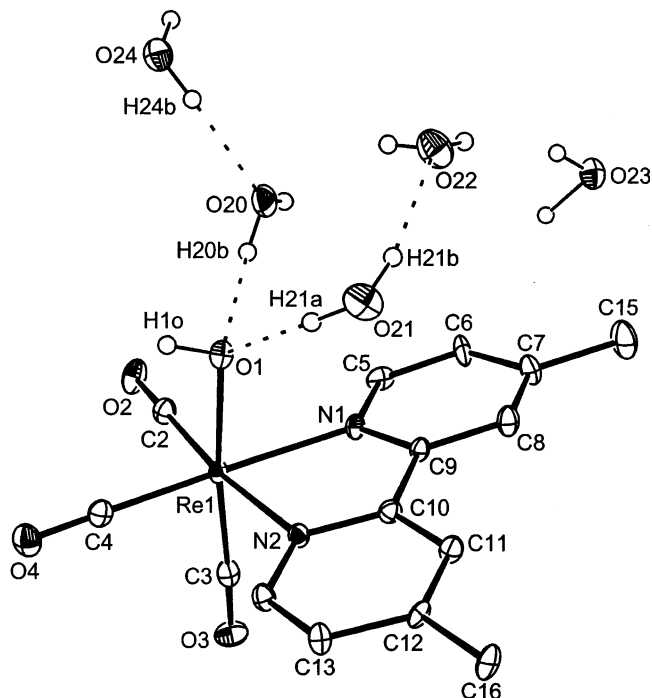


Figure 1. ORTEP drawing of **8a** with thermal ellipsoids shown at the 50% probability level.

angle of 165.5(14)°. Each of these water molecules interacts with another water through hydrogen bonding, thus forming an extensive intermolecular network that involves the OH of the complex and four waters of solvation. A fifth and final water molecule in the crystal lattice does not appear to interact with the others. Chemically, **8a** and **8b** appear to behave in the same way; however, the reactions reported herein were conducted with **8b** to minimize water in the reaction mixtures.

Compound **18** can be prepared by oxidation of formyl complex **4** or from **5** as described above. It was characterized by elemental analysis, ¹H and ¹³C NMR and IR spectroscopy, and X-ray crystallography. The ORTEP diagram for **18** is shown in Figure 2; crystallographic data are shown in Table 1, and selected bond distances and bond angles are shown in Table 3. The structure shows slightly distorted octahedral geometry about each of the three equivalent rhenium centers, with the trans C–Re–O bond angles varying from 171.0(3)° for C(10)–Re(3)–O(3) to 176.6(2)° for C(7)–Re(2)–O(2); distortion

Table 1. Crystal Data and Refinement Parameters for 8a and 18

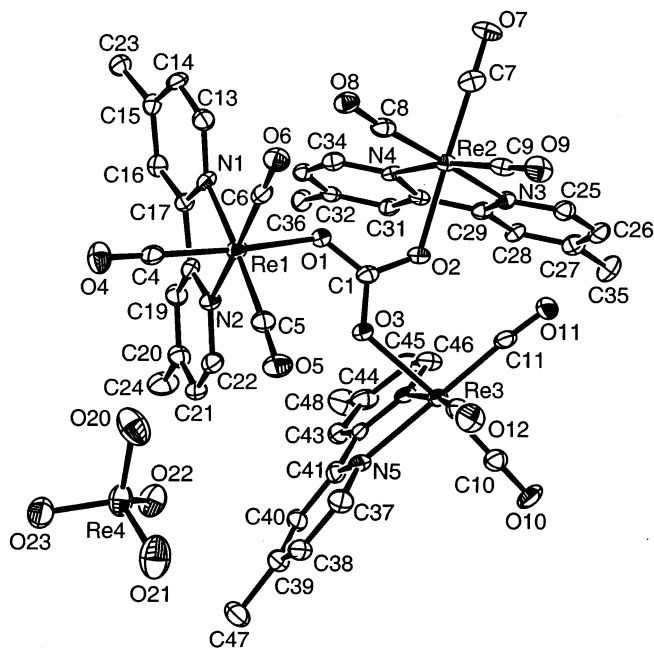
	8a	18
empirical formula	C ₁₅ H ₁₃ N ₂ O ₄ Re·5H ₂ O	C ₄₈ H ₄₈ N ₆ O ₁₂ Re ₃ ⁺ ReO ₄ ⁻ ·0.75CH ₂ Cl ₂ ·0.5(CH ₃ CH ₂) ₂ O
fw	561.55	1776.8
cryst syst	monoclinic	monoclinic
space group	C2/c	C2/c
a, Å	38.655(5)	40.977(5)
b, Å	12.647(2)	13.106(2)
c, Å	8.514(1)	23.985(3)
α, deg	90	90
β, deg	95.985(2)	123.571(2)
γ, deg	90	90
V, Å ³	4139.2(9)	10732(2)
Z	8	8
D _{calcd} , mg/m ³	1.802	2.199
μ, mm ⁻¹	5.918	9.143
θ range, deg	1.70–28.23	1.66–28.22
no. of rflns measd	17 110	45 501
no. of unique rflns (R _{int})	4635 (0.038)	12 472 (0.049)
GOF	1.061	1.028
R1, wR2 (I > 2σ(I)) ^a	0.032, 0.082	0.039, 0.103
R1, wR2 (all)	0.034, 0.083	0.052, 0.111

$$^a R1 = \sum |F_o| - |F_c| / \sum |F_o|; wR2 = \{ \sum [w(F_o^2 - F_c^2)^2] / \sum [w(F_o^2)^2] \}^{1/2}.$$

Table 2. Selected Bond Distances (Å) and Angles (deg) for 8a

Bond Distances			
Re–C(2)	1.912(4)	C(2)–O(2)	1.163(5)
Re–C(3)	1.907(4)	C(3)–O(3)	1.169(5)
Re–C(4)	1.921(4)	C(4)–O(4)	1.157(5)
Re–O(1)	2.132(3)	O(1)–H(10)	0.86(6)
Re–N(1)	2.179(3)	O(1)–H(21a)	1.92(6)
Re–N(2)	2.183(3)	O(1)–H(20b)	1.78(6)
Bond Angles			
C(3)–Re–C(2)	88.22(16)	O(1)–Re–N(1)	79.90(11)
C(3)–Re–C(4)	89.70(17)	C(3)–Re–N(2)	93.92(14)
C(2)–Re–C(4)	88.69(17)	C(2)–Re–N(2)	173.40(15)
C(3)–Re–O(1)	173.95(13)	C(4)–Re–N(2)	97.55(15)
C(2)–Re–O(1)	95.58(14)	O(1)–Re–N(2)	81.79(11)
C(4)–Re–O(1)	95.07(14)	N(1)–Re–N(2)	74.85(12)
C(3)–Re–N(1)	94.90(15)	O(2)–C(2)–Re	178.7(3)
C(2)–Re–N(1)	98.76(15)	O(4)–C(4)–Re	178.7(4)
C(4)–Re–N(1)	171.34(14)	O(3)–C(3)–Re	177.5(4)
O(1)–H(21a)–O(21)	163.9(15)	O(1)–H(20b)–O(2)	165.5(14)

is caused by the small bite angle of the dmbpy ligands (around 75° rather than the ideal 90°). Bonding around the carbonato group is very symmetrical; the Re–O bond lengths, 2.131(4)–2.132(4) Å, are the same within experimental error, while the carbonato C–O bond lengths range from 1.277(8) to 1.299(8) Å. Slightly distorted tetrahedral geometry is shown around rhenium in ReO₄⁻ with the O–Re–O bond angles varying from 107.4(4) to 111.7(3)°. Compound **18** is similar to the carbonato-bridged compound {[Re(CO)₅]₃OCO₂}[ReO₄], which cocrystallized with [Re(CO)₃(OH)]₄ from a reaction mixture containing (η²-C₂H₄)Re(CO)₅⁺ that had been exposed to air.¹³ There is more variation in the C–O bond distances in the carbonato ligand of the cation in Beck's compound, 1.273(41)–1.311(43) Å, than in **18** and more variation in the O–C–O bond angles, 118.2(29)–121.3(31)°, than those in **18**, which are all close to 120°.

**Figure 2.** ORTEP drawing of **18** with thermal ellipsoids shown at the 50% probability level.**Table 3. Selected Bond Distances (Å) and Bond Angles (deg) for 18**

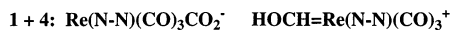
Bond Distances			
Re(1)–C(4)	1.895(7)	O(3)–C(1)	1.288(8)
Re(1)–O(1)	2.132(4)	O(4)–C(4)	1.163(9)
Re(2)–C(7)	1.902(8)	O(7)–C(7)	1.152(9)
Re(2)–O(2)	2.131(4)	O(10)–C(10)	1.160(9)
Re(3)–C(10)	1.891(8)	Re(4)–O(20)	1.699(7)
Re(3)–O(3)	2.132(4)	Re(4)–O(21)	1.685(8)
O(1)–C(1)	1.278(8)	Re(4)–O(22)	1.691(6)
O(2)–C(1)	1.277(8)	Re(4)–O(23)	1.715(6)
Bond Angles			
C(4)–Re(1)–O(1)	172.5(3)	O(2)–C(1)–O(1)	120.3(6)
C(6)–Re(1)–O(1)	93.3(2)	O(2)–C(1)–O(3)	119.6(6)
C(5)–Re(1)–O(1)	97.3(3)	O(1)–C(1)–O(3)	120.2(6)
O(1)–Re(1)–N(2)	84.1(2)	O(4)–C(4)–Re(1)	178.9(8)
O(1)–Re(1)–N(1)	81.3(2)	O(5)–C(5)–Re(1)	178.0(7)
N(2)–Re(1)–N(1)	74.8(2)	O(6)–C(6)–Re(1)	178.9(7)
C(7)–Re(2)–O(2)	176.6(2)	O(21)–Re(4)–O(22)	111.6(3)
C(10)–Re(3)–O(3)	171.0(3)	O(21)–Re(4)–O(20)	107.4(4)
N(4)–Re(2)–N(3)	74.8(2)	O(22)–Re(4)–O(20)	109.5(3)
N(5)–Re(3)–N(6)	74.6(2)	O(21)–Re(4)–O(23)	111.7(3)
C(1)–O(1)–Re(1)	128.4(4)	O(22)–Re(4)–O(23)	107.8(3)
C(1)–O(2)–Re(2)	125.2(4)	O(20)–Re(4)–O(23)	108.8(3)
C(1)–O(3)–Re(3)	124.0(4)		

The bridging hydride **11** (with a triflate anion) can be generated, in situ, by the reaction of hydride **6** with **9a** in DMF-*d*₇, but the compound proved difficult to isolate. However, reaction of **6** and **9a** in CH₂Cl₂ showed that **11** was formed in about 60% yield, but only a much smaller amount of it could be isolated in pure form. Elemental analysis and ¹H NMR spectral data support its formulation; also, the hydride resonance appears at δ –8.77 in CD₂Cl₂, which compares favorably with that reported for *fac, fac*-[Re(bpy)(CO)₃HRe(bpy)(CO)₃][Cl] (δ –8.76 in CD₂Cl₂).^{1d}

Hydroxo compound **17** was prepared in the same way that we prepared **8b**.^{2a} Treatment of *fac*-[Re(bpy)(CO)₃Otf] (**16**) with aqueous KOH afforded **17**; the crude product was washed with water and then dried under high vacuum. It was characterized by elemental analysis and by IR and ¹H NMR data.

(13) Breimair, J.; Robl, C.; Beck, W. *J. Organomet. Chem.* **1991**, *411*, 395.

Scheme 6



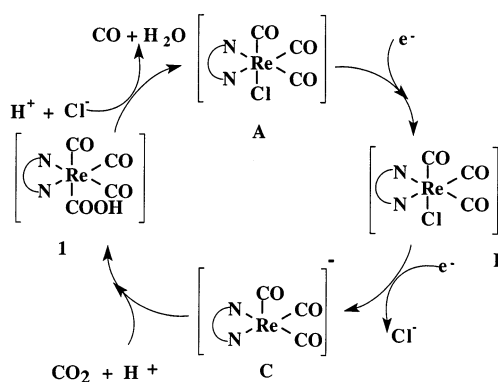
An authentic sample of **13** was prepared by reaction between equimolar quantities of cation **9a** and **17**, thus showing that a hydroxo ligand can add to a metal carbonyl group.⁶ The product was characterized by elemental analysis and by IR and ¹H NMR spectral data, which are consistent with its formulation as the CO₂-bridged compound *fac, fac*-[Re(dmbpy)(CO)₃CO₂Re-(bpy)(CO)₃]; it showed IR ν_{OCO} bands at 1486 (w) and 1153 (m) cm⁻¹, which are similar to the corresponding bands for **2** (1485 (w) and 1155 (m) cm⁻¹).^{2a}

(f) Intermediates Formed in the Reactions of 1.

The intermediate species observed in reactions of **1** alone or those involving **4**, **6**, and **8b** also show very similar ¹H NMR spectral patterns. The low-field resonances for the polypyridyl ring protons show broadening of resonances at δ 8.45 and 7.41 in DMF-*d*₇; otherwise, the resonances are at the same chemical shift positions and show multiplicities such as those of the CO₂-bridged compound **2**: δ 8.61(d), 8.48 (d), 8.45 (s), 8.26 (s), 7.41 (d), and 7.25 (d). However, in the cases of intermediates formed from **1** with **4** or from **1** with **6**, there is some broadening of the resonances at δ 8.61, and the intensity of the resonance at δ 7.41 is reduced as well. The broadening is suggestive of dynamic behavior, but the data also suggest the presence of similar species. It is worth noting that there is nothing unusual about the behavior of compound **2** in solution by itself; also, treating DMF-*d*₇ solutions of **2** with N₂, in the manner of the reactions of **1** described above, does not change the ¹H NMR spectrum in any way. After obtaining ¹H NMR spectra of the mixed CO₂-bridged compound **13**, we could determine that the broadened peaks in the intermediates were on the "oxygen side" of the CO₂ bridge in compound **2**. Also, the degree of broadening is somewhat different among the intermediates: **1** + **6** > **1** + **4** > **1** + **8b** \approx **1**. The formation of ion pairs, such as those represented in Scheme 6, is appealing as a possible explanation for the similarity of the ¹H NMR spectra of the intermediates, since the carboxylate anion would be common to all of them and the cationic portions could be expected to have chemical shifts similar to those on the oxygen side of the CO₂ bridge in **2**. If this is correct, the species certainly behave in separate ways upon quenching, since totally different product mixtures are obtained.

(g) Relation of These Results to the Photocatalytic Reactions. The reactions of **1** and **4** reported here, and those of compounds which could be derived from them in the catalytic reactions, are best explained as resulting from complex, competing equilibria. At least two reaction pathways are open to the metalloacid **1**: (a) ionization to $\text{Re}(\text{dmbpy})(\text{CO})_4^+$ and OH⁻, which could be followed by conversion to *fac*-[Re(η^1 -dmbpy)(CO)₄OH] as suggested in Scheme 2, and (b) proton transfer to a basic species, as shown in Schemes 1 and 4. This versatility, and the ability of **1** to participate in several of equilibria, are believed to be responsible for many of the transformations which occurred in our reactions.

Scheme 7



Formyl complex **4**, although not highly labile alone, is very labile in the presence of **1**. This may be attributed to the ability of **4** to transfer hydride to **1** or to its ability to behave as a proton acceptor at the formyl oxygen.⁹

The cycle shown in Scheme 7 is the one suggested some time ago by Ziesel^{1e} for the photocatalytic reductions of CO₂ involving *fac*-[Re(N-N)(CO)₃Cl] (N-N = bipyridine ligand). Anions of type C in Scheme 7, and likely key intermediates, have been suggested as products of electrochemical reductions of the corresponding chlorides (N-N = bpy^{1g} or dmbpy^{1f,h}) as the result of analyses of in situ infrared spectral data. However, these suggestions have not led to firm characterizations of these anions. Competition for C by CO₂ and H⁺ would determine whether a hydride (e.g., **6**) or metalloacid (e.g., **1**) were formed; where N-N = 4,4'-dimethyl-2,2'-bipyridine, **6** would certainly produce formate **7** in the presence of CO₂. The speed with which **1** was converted to bicarbonato complex **3** in the presence of CO₂ suggests that a metalloacid would not have a long lifetime in the catalytic reactions (bicarbonate was not reported^{1e}). Thus, the metalloacid may be quickly converted to $\text{Re}(\text{N-N})(\text{CO})_4^+$ under photocatalytic conditions (by ionization or by acid-promoted dehydroxylation) and then partition between paths leading to CO or to formate plus CO. We showed previously that conversion of $\text{Re}(\text{dmbpy})(\text{CO})_4^+$ to *fac*-[Re(dmbpy)(CO)₃Cl] (and, presumably, CO) occurs rapidly upon photolysis in the presence of Cl⁻.³ We have argued that the conditions available in the photocatalytic reactions are conducive to the generation of formyl complexes from $\text{Re}(\text{N-N})(\text{CO})_4^+$, and we demonstrated that formyl complex **4** will transfer hydride to CO₂, yielding [Re(dmbpy)(CO)₄][O₂CH] rapidly.³ This ionic formate is quickly converted to **7** (with liberation of CO). Also, the reduction potentials of *fac*-[Re(dmbpy)(CO)₄][OTf] (**9a**) and *fac*-[Re(dmbpy)(CO)₃Cl] are similar ($E_{1/2} = -1.30^4$ and -1.43 V,¹⁴ respectively). Our proposal fits the condition noted by Ziesel^{1e} that CO and formate are formed by parallel, not consecutive, paths.

Experimental Section

General Data. Reagent grade benzene, dichloromethane, acetone, and dimethyl sulfoxide and HPLC grade hexane were used as received. Diethyl ether was distilled from sodium benzophenone. DMF-*d*₇, DMSO-*d*₆, and CD₂Cl₂ were obtained from Cambridge Isotope Laboratories and used as received.

(14) Breikss, A. I.; Abruña, H. D. *J. Electroanal. Chem. Interfacial Electrochem.* **1986**, *201*, 347.

2,2'-Bipyridine and 4,4'-dimethyl-2,2'-bipyridine were obtained from Aldrich and used as received. Samples of *fac*-[Re(dmbpy)-(CO)₃COOH] (**1**),^{2a} *fac, fac*-[Re(dmbpy)(CO)₃CO₂] (**2**),^{2a} *fac*-[Re(dmbpy)(CO)₃O₂COH] (**3**),^{2b} *fac*-[Re(dmbpy)(CO)₃CHO] (**4**),³ *fac*-[Re(dmbpy)(CO)₃H] (**6**),^{2a,8} *fac*-[Re(dmbpy)(CO)₃OCHO] (**7**),^{2a,8} *fac*-[Re(dmbpy)(CO)₃OH·H₂O] (**8b**),^{2a} *fac*-[Re(dmbpy)(CO)₄]-[OTf] (**9a**),⁴ *fac*-[Re(dmbpy)(CO)₄][BF₄] (**9b**),⁴ *fac, fac*-[Re(dmbpy)(CO)₃]₂ (**10**),⁵ *fac*-[Re(bpy)(CO)₃H] (**12**),⁸ *fac*-[Re(bpy)-(CO)₃OCHO] (**14**),⁸ *fac*-[Re(dmbpy)(CO)₃(OTf)] (**15**),^{2a} and *fac*-[Re(bpy)(CO)₃(OTf)] (**16**)⁴ were prepared as described previously. Spectral data were obtained on the following instruments: NMR, Varian Unity Inova 500 MHz; FTIR, Mattson, RS-1. Diffuse reflectance data were obtained on the Mattson instrument with a DRIFTS accessory (Graseby Specac Inc., "Mini-Diff") as KCl dispersions. ¹H and ¹³C NMR spectra were referenced to residual protons in the deuterated solvents. Glovebox experiments were conducted in a Vacuum Atmospheres glovebox, fitted with a DriTrain, under dry nitrogen. Gas chromatographic analyses were conducted on a Buck Scientific Model 910 instrument with a thermal conductivity detector and a 6 foot × 1/8 in. molecular sieve 5A column. Melting points were obtained on a Thomas-Hoover capillary melting point apparatus and are uncorrected. Elemental analyses were performed by Midwest Microlab, Indianapolis, IN.

Reactions of 1 and 2 with CO₂. Solutions of CO₂ in DMSO-*d*₆ were prepared as follows: a 50 mL distilling flask with a sidearm and stopcock and a rubber septum was filled with CO₂ and then taken into the glovebox, where 1.2 mL of DMSO-*d*₆ was added through the septum. The mixture was then stirred for 1 h to saturate the solvent with CO₂.

(a) Reaction of 1. In the glovebox, the CO₂-saturated solution was transferred to an NMR tube containing 5 mg of **1**, which was closed and inverted to mix the contents, and then the sample was monitored over time by ¹H NMR. After 10 min, the composition was 42% bicarbonate compound **3** and 58% unreacted **1**. After 20 min, the composition was 70% **3** and 30% **1**. After 40 min, the composition was 87% **3**, 8% **1**, and 4% **5**.

(b) Reaction of 2. In the glovebox, the CO₂-saturated solution was transferred to an NMR tube containing 6 mg of **2**, which was closed and inverted to mix the contents, and then the sample was monitored over time by ¹H NMR. After 10 min, the composition was 21% **3**, 15% **1**, and 64% unreacted **2**. After 20 min, the composition was 38% **3**, 11% **1**, and 51% unreacted **2**. After 40 min, the composition was 70% **3**, 3% **1**, and 27% unreacted **2**; no **5** was visible.

Reactions Involving 1. In each of the experiments summarized below, the samples (typically containing about 4 mg of **1** together with equimolar amounts of the second compound) were prepared in a glovebox under N₂ and in degassed DMF-*d*₇ with ferrocene as an internal standard. In reactions **b–d**, a reaction intermediate appeared which had ¹H NMR spectral properties that were closely similar to those of the intermediate generated in reactions of **1** alone. After this intermediate appeared, and the peaks for starting materials had disappeared, reactions were quenched by pouring the NMR sample into a flask filled with dry N₂ and then the mixture was reanalyzed by ¹H NMR. Product compositions are reported in mole percentages.

(a) Reaction of 1. The reaction was quenched after 40 min; ¹H NMR analysis showed that the product mixture consisted of 68% **2**, 10% **3**, 3% **10**, and 3% free dmbpy.

(b) Reaction of 1 with 4. The reaction was quenched after 1 h 40 min; the composition of the mixture was: 29% **2**, 22% **7**, 30% **6**, 11% **11**, 5% free dmbpy, and about 1% of **10**.

(c) Reaction of 1 with 6. The reaction required 3 h; the product mixture consisted of the following compounds: **2** (18%), **7** (19%), **6** (46%), [*fac*-Re(dmbpy)(CO)₃]₂H⁺ (**11**, 9%), identified by comparison of the ¹H NMR spectrum with that

of the compound generated from the reaction of **6** with **9a**; see below), free dmbpy (4%), and a trace of **10**.

(d) Reaction of 1 with 8b. The reaction was started at 0 °C and then warmed to 25 °C and quenched with N₂; the ¹H NMR spectrum showed a product mixture consisting of the following compounds: 54% **2**, 14% **5**, 7% **10**, and 3% dmbpy together with a trace amount of **3**.

(e) Reaction of 1 with 12. After quenching, the new product mixture consisted of *fac, fac*-Re(dmbpy)(CO)₃CO₂Re(bpy)(CO)₃ (**13**; 24%, identified by comparison with an authentic sample; see below), hydride **6** (17%), **7** (8%), **12** (17%), *fac*-Re(bpy)(CO)₃OCHO (**14**, 9%), **2** (5%), and smaller amounts of several other compounds, including **11**.

Reaction of 4 Alone. In the manner described above for reactions involving **1**, a solution with 3 mg of **4** in degassed DMF-*d*₇ containing ferrocene as internal standard was prepared in the glovebox and sealed in an NMR tube. After 1 h, NMR analysis showed that the mixture consisted of 95% unreacted **4** and 5% **1**. After 3 h, the mixture consisted of 83% **4**, 7% **1**, 3% **2**, and smaller amounts of **6** and **7**.

GC Analyses of the Gases Liberated from the Reactions of 1 with and without 4. For GC detection of H₂, nitrogen was used as the carrier gas at a flow rate of 20 mL/min (11 psi), operating at a column oven temperature of 36 °C and a detector temperature of 61 °C. Analysis showed H₂ as a negative peak with retention time of 0.45 min. For CO detection, helium gas was used as the carrier gas at a flow rate of 20 mL/min (11 psi). CO was detected at 8.92 min.

To a flask containing **1** (65 mg, 0.13 mmol) was added degassed DMF-*d*₇ (5 mL) in the glovebox, and the flask was sealed with a septum. The acid was dissolved and allowed to stand for 19 h, giving a dark red solution. The ¹H NMR spectrum of the solution showed it consisted of **2** (75%), **5** (14%), and small amounts of other products. GC analysis of the headspace gases indicated no H₂, but CO was detected (0.074 mmol).

The reaction of **1** (44 mg) with **4** (41 mg) was conducted similarly and allowed to stand for 3 days to go to completion. Headspace analysis (via a sample withdrawn by gastight syringe) showed a small peak for H₂; the yield was estimated as 3% (based on **1**).

{*fac, fac*-[Re(dmbpy)(CO)₃]₂(OCO₂)} (**5**). To a flask containing 9 mL of degassed DMSO was added **3** (51 mg, 0.1 mmol) and **1** (51 mg, 0.1 mmol). The reaction mixture was stirred for 5 min and then left at room temperature for 3.5 h; a yellow solid precipitated during this time. The yellow solid was collected by filtration, washed with ether and hexane, and dried under high vacuum. Yield: 64 mg (65%).

Anal. Calcd for C₃₁H₂₄N₄O₉Re₂: C, 38.43; H, 2.50; N, 5.78. Found: C, 38.21; H, 2.48; N, 5.59. IR (DRIFTS, KCl): ν_{CO} 2024, 1893, 1852; ν_{OCO} 1575, 1483, 1269 cm⁻¹. ¹H NMR (DMF-*d*₇): δ 8.70 (2H, d), 8.21 (s), 7.34 (d), 2.25 (s). ¹H NMR (CD₂Cl₂): δ 8.84 (d), 7.98 (s), 7.31 (d), 2.55 (s).

fac-[Re(dmbpy)(CO)₃OH]·2.5H₂O (**8a**). The synthesis of the orange hydroxy compound *fac*-[Re(dmbpy)(CO)₃OH]·H₂O (**8b**) was reported previously.^{2a} When the orange compound was dissolved in acetone, it gave a red-orange solution. Addition of water to this solution caused a change in color to yellow, from which yellow crystals were obtained after concentration. The yellow crystals, collected by filtration and air-dried overnight, showed IR and NMR spectra that were indistinguishable from those of the orange compound.

Anal. Calcd. for C₁₅H₁₃N₂O₄Re·2.5H₂O: C, 34.88; H, 3.51. Found: C, 34.93; H, 3.53.

{*fac, fac*-[Re(dmbpy)(CO)₃]₂H}[OTf] (**11**). (a) To an NMR tube containing a mixture of **6** (4.1 mg, 0.009 mmol) and **9a** (5.5 mg, 0.009 mmol) was added 2 mL of degassed DMF-*d*₇ in the glovebox. The NMR tube was sealed and moved out of the glovebox, and then the reaction was monitored by ¹H NMR spectroscopy. The spectrum revealed that **11** was being formed. After 80 min, the tube was returned to the N₂-filled glovebox

and the solution poured into a flask. The solution was stirred for 5 min and then transferred back to the NMR tube. The spectrum showed that the solution contained 80% **11** and 20% unreacted **6**; **9a** was not observed. The ¹H NMR spectrum of **11** in DMF-*d*₇ showed signals at δ 8.53 (d), 8.36 (s), 7.53 (d), 2.66 (s), and -8.53 (s, hydride proton).

(b) A mixture of **6** (100 mg, 0.22 mmol) and **9a** (120 mg, 0.20 mmol) was dissolved in 20 mL of CH₂Cl₂ in a flask inside the glovebox. The flask was sealed and removed from the glovebox. The reaction mixture was kept 0 °C for 3 days. Then, a portion of the mixture was evaporated to dryness, the residue was taken up in CD₂Cl₂, and the ¹H NMR spectrum was recorded. Analysis showed that **6** had been consumed and the bridging hydride constituted 56% (mol %) of the sample. The remainder of the reaction mixture was filtered, and solvent was evaporated from the filtrate. The residue was then recrystallized twice from acetone/hexane to give the pure product (76 mg, 31%) as yellow needles, mp 230–232 °C dec.

Anal. Calcd for C₃₁H₂₅F₃N₄O₉Re₂S·2C₃H₆O·2H₂O: C, 36.69; H, 3.41. Found: C, 36.64; H, 3.52. IR (DRIFTS, KCl): ν_{CO} 2032 (s), 2017 (s), 1919 (vs). ¹H NMR (CD₂Cl₂): δ 8.44 (δ), 8.11 (s), 7.21 (d), and -8.77 (s); resonances for acetone and water were observed in the ¹H NMR spectrum also.

fac, fac-[Re(dmbpy)(CO)₃CO₂Re(bpy)(CO)₃] (13). A mixture of **17** (0.033 g, 0.074 mmol) and **9b** (0.048 g, 0.084 mmol) in acetone (40 mL) and water (0.5 mL) was stirred under nitrogen at 0 °C for 70 min. The mixture was warmed to room temperature and then stirred for 3 h. The red solid which precipitated was washed with acetone and dried under high vacuum to give the product *fac, fac*-[Re(dmbpy)(CO)₃CO₂Re(bpy)(CO)₃], mp 225–229 °C dec. Yield: 0.022 g (32%).

Anal. Calcd for C₂₉H₂₀N₄O₈Re₂·H₂O: C, 36.94; H, 2.35. Found: C, 36.69; H, 2.43. IR (DRIFTS, KCl): ν_{CO} 2002 (s), 1993 (s), 1891 (b, s); ν_{OCO} 1486 (w), 1153 (m) cm⁻¹. ¹H NMR (DMSO-*d*₆): δ 8.67 (2H, d, *J* = 5.5 Hz), 8.47 (2H, d, *J* = 8.5 Hz), 8.35 (2H, d, *J* = 5.5 Hz), 8.22 (2H, t, *J* = 7.5 Hz), 8.13 (2H, s), 7.50 (2H, t, *J* = 6 Hz), 7.17 (2H, d, *J* = 6 Hz), 2.53 (6H, s). The water content in the product was established by ¹H NMR analysis of the sample in DMSO-*d*₆ using ferrocene as internal standard.

fac-[Re(bpy)(CO)₃OH] (17). A mixture of *fac*-Re(bpy)-(CO)₃OTf (**16**; 0.40 g, 0.70 mmol) and KOH (6 mL of 4 M solution) in acetone (40 mL) and water (30 mL) was refluxed for 20 h to give a red solution. The solution was cooled to room temperature and then concentrated to precipitate a yellow solid. The solid was collected by filtration, washed with water, and dried under high vacuum to give the orange-red product, mp 169–171 °C dec. Yield: 0.19 g, 61%.

Anal. Calcd for C₁₃H₉N₂O₄Re: C, 35.21; H, 2.5. Found: C, 34.95; H, 2.11. IR (DRIFTS, KCl): ν_{CO} 2000 (s), 1881 (s), 1858 (vs) cm⁻¹. ¹H NMR (CD₂Cl₂): δ 9.01 (2H, d, *J* = 4 Hz), 8.24 (2H, d, *J* = 8.5 Hz), 8.09 (2H, t, *J* = 7.5 Hz), 7.54 (2H, t, *J* = 5 Hz).

{*fac, fac, fac*-[Re(dmbpy)(CO)₃]₃(OCO₂)}[ReO₄] (**18**).

A suspension of **4** (0.29 g, 0.6 mmol) in benzene (30 mL) was purged with O₂ for 1 h and then stirred overnight. The mixture was evaporated to dryness, and the residue was triturated with CH₂Cl₂ and hexane, leaving a yellow precipitate, mp > 230 °C. Yield: 0.090 g, 36%.

Anal. Calcd for C₄₆H₃₆N₆O₁₆Re₄: C, 33.01; H, 2.17. Found: C, 33.31; H, 2.29. IR (DRIFTS, KCl): ν_{CO} 2022 (s), 1918 (s), 1895 (s), 1886 (s), 1869 (s) cm⁻¹; ν_{OCO} 1442, 1421 cm⁻¹; ν_{ReO} 909 cm⁻¹. ¹H NMR (DMF-*d*₇): δ 8.76 (s), 8.40 (d), 7.60 (d), 2.63 (s). ¹H NMR (CD₂Cl₂): δ 8.51 (2H, d), 8.10 (2H, s), 7.28 (2H, d), 2.60 (6H, s). ¹³C NMR (DMF-*d*₇): δ 198.43, 194.62, 167.97, 156.26, 153.52, 153.00, 128.85, 125.33, 21.21.

Conversion of 5 to 18. To a solution of **15** (0.031 g, 0.051 mmol) in CH₂Cl₂ (35 mL) was added compound **5** (0.480 g, 0.050 mmol). The resulting suspension was stirred overnight, giving a clear yellow solution. After the solution was concentrated to 5 mL, hexane (30 mL) was added to precipitate the

product, yield 0.076 g, 97%. To a solution of this product in acetone was added a 3-fold excess of NH₄ReO₄ in water; the yellow solid which precipitated had exactly the same spectral properties as the product from the method above.

X-ray Crystal Structure of 8a and 18. Data were collected using graphite-monochromated Mo Kα radiation from a sealed, ceramic tube equipped with a monocapillary. SMART (version 5.625)¹⁵ was used for preliminary determination of the cell constants and data collection control. Determination of integral intensities and global cell refinement were performed with the Bruker SAINT (version 6.22)¹⁶ software package using a narrow-frame integration algorithm. Semiempirical absorption corrections were applied on the basis of the intensities of symmetry-related reflections measured at different angular settings using SADABS (version 2.02).¹⁷ Thermal ellipsoid representations for **8a** and **18** were prepared using ORTEP-3.¹⁸

Crystals of **8a** suitable for X-ray analysis were obtained by dissolving the orange complex in acetone, adding an equal volume of water, and allowing the sample to stand under nitrogen for 2 days. A yellow plate (0.29 mm × 0.15 mm × 0.03 mm) of **8a** was mounted on a 10 μm, 0.10 mm CryoLoop, and data were collected at 100 K on a Bruker Smart APEX CCD diffractometer. A full sphere of data was collected in 1868 frames at an exposure time of 15 s per frame. The structure was solved by heavy-atom Patterson methods and refined using SHELXTL.¹⁹ All non-hydrogen atoms were refined anisotropically. The hydroxyl hydrogen atom was located by a difference map and was refined isotropically. Methyl and phenyl hydrogen atoms were determined geometrically and allowed to ride on attached carbon atoms as fixed contributions. In addition, five water molecules which form an extensive hydrogen-bonding network are present (see Figure 1). Difference maps were used to determine the locations for hydrogen atoms in each H₂O molecule. Their positions were refined. For all 4635 reflections (*R*(int) = 0.038), the final anisotropic full-matrix least-squares refinement on *F*² for 280 variables converged at *R*1 = 0.032 and *wR*2 = 0.083 with a GOF of 1.06.

Crystals of **18** suitable for X-ray diffraction experiments were grown by slow diffusion of ether into CH₂Cl₂ solution. A thin yellow plate (0.40 mm × 0.11 mm × 0.02 mm) of **18** was mounted on a 10 μm, 0.10 mm CryoLoop, and data were collected at 100 K on a Bruker Smart APEX CCD diffractometer. A full sphere of data was collected in 1868 frames at an exposure time of 30 s per frame. The structure was solved by heavy-atom Patterson methods (XS) and refined (XL) using the Bruker SHELXTL (version 6.12)¹⁹ program suite. All non-hydrogen atoms of the cation and anion were refined anisotropically. A 75% occupancy methylene chloride solvate was refined anisotropically without including hydrogen atoms. A partial ether solvate having an occupancy of 25% was refined isotropically; hydrogen atoms of the solvate were excluded. For hydrogen atoms in the cation, a riding model was employed under restriction of ideal geometry and included as fixed contributions (*B* = 1.2 (phenyl) and 1.5 (methyl) times the value for the corresponding attached carbon atom). For all 12 472 reflections (*R*(int) = 0.049), the final anisotropic full-matrix least-squares refinement on *F*² for 704 variables converged at *R*1 = 0.039 and *wR*2 = 0.111 with a GOF of 1.03.

(15) SMART, version 5.625; Bruker Advanced X-ray Solutions, Madison, WI, 2002.

(16) SAINT, version 6.22; Bruker Advanced X-ray Solutions, Madison, WI, 2001.

(17) Sheldrick, G. M. SADABS: Area Detector Absorption Correction; University of Göttingen, Göttingen, Germany, 1997.

(18) Farrugia, L. J. ORTEP-3 for Windows. *J. Appl. Crystallogr.* **1997**, *30*, 565.

(19) SHELXTL, version 6.12: Program Library for Structure Solution and Molecular Graphics; Bruker Advanced X-ray Solutions, Madison, WI, 2001.

Acknowledgment. This work was supported by the United States Department of Energy, Division of Chemical Sciences, Office of Science (Grant No. DE-FG02-86ER13538), and by the National Science Foundation (Grant No. CHE-0203131). The CCD X-ray equipment was purchased through funds from the Kentucky Research Challenge Trust Fund.

Supporting Information Available: Tables giving full details of the crystallographic data and data collection parameters, atom coordinates, bond distances and bond angles, anisotropic thermal parameters, and hydrogen coordinates for **8a** and **18**. This material is available free of charge via the Internet at <http://pubs.acs.org>.

OM020677Q